J Fluoresc
DOI 10.1007/s10895-013-1320-9

ORIGINAL PAPER

Spectroscopy and Photophysics of Monomethyl-Substituted Derivatives of 5-Deazaalloxazine and 10-Ethyl-5-Deaza-Isoalloxazine

Dorota Prukała · Magdalena Taczkowska · Mateusz Gierszewski · Tomasz Pędziński · Marek Sikorski

Received: 9 June 2013 / Accepted: 7 November 2013

Abstract Steady-state and time-resolved spectra were used to describe the singlet and triplet states of 8-methyl-5-deazaalloxazine (8-Me-5-DAll), 9-methyl-5-deazaalloxazine (9-Me-5-DAll) and 10-ethyl-5-deaza-isoalloxazine (10-Et-5-DIAll). Solvatochromic properties were described using different polarity scales, including Δf and the four-parameter scale proposed by Catalán. The results indicate that the Catalán scale shows a strong influence of solvent acidity (hydrogen-bond donating ability) on the emission properties of 8-Me-5-DAll and 9-Me-5-DAll. These results indicate the importance of intermolecular solute-solvent hydrogen-bonding interactions in the excited state of these compounds. Contrary to deazaalloxazines, solvent acidity affects the absorption spectra of 10-Et-5-DIAll. Fluorescence lifetimes and quantum yields and also transient absorption spectra were determined for all of the compounds studied. Electronic structure and S_0-S_i, S_0-T_i, T_1-T_i transitions energies and oscillator strengths were calculated using the TD-DFT methods. Theoretical calculations were compared to experimental data.

Keywords 5-deazaalloxazine · 5-deaza-isoalloxazine · TD-DFT study · Photophysics · Spectroscopy · Transient absorption spectra

Electronic supplementary material The online version of this article (doi:10.1007/s10895-013-1320-9) contains supplementary material, which is available to authorized users.

D. Prukała (✉) · M. Taczkowska · M. Gierszewski · T. Pędziński · M. Sikorski
Faculty of Chemistry, A. Mickiewicz University, Umultowska 89B, 61-614 Poznań, Poland
e-mail: dprukala@amu.edu.pl

Present Address:
M. Taczkowska
FT/ICR MS Laboratory, Department of Earth Sciences, The University of Hong Kong, Hong Kong, Hong Kong

Introduction

Flavins are known for their important role in various biological systems [1–3]. Different light-induced reactions of flavins (riboflavin—RF, flavin mononucleotide—FMN, and flavin adenine nucleotide—FAD) in the various photosensory pigments, including covalent bond formation, stable radical formation, hydrogen bond rearrangements, and electron transfer [4] have been detected. 5-Deazaflavins are analogues of flavins. Literature shows that 5-deazaflavin derivatives, including enzyme systems, so far believed to be strictly limited to the *Archaea* kingdom of life, are far more widespread than anticipated [5]. Photophysical properties of flavins (isoalloxazines) and 5-deazaflavins (5-deaza-isoalloxazines) are similar in many aspects.

5-Deaza-flavins are cofactors in yellow chromophores [6] and are known as blue-light receptors [6, 7]. They are potential riboflavin antagonists with their own redox system, different from that of riboflavin [8]. Recently, 5-deazaflavin (5-deaza-isoalloxazine) and its homologues with the 5-deazaalloxazine structure were reported having antitumor activity in vitro [9–13]. It was also reported that in *Mycobacterium tuberculosis*, F_{420}-dependent enzymes are involved in metabolic activation of some antitubercular compounds [14].

Derivatives of 5-deazalloxazines unsubstituted at the N(1) position can undergo excited-state proton transfer (ESDPT) from N(1) to N(10). This reaction occurs in the presence of compounds with donor-acceptor properties such as carboxylic acids, e.g. acetic acid. It was investigated by Koziołowa for 5-deazalumichrome (7,8-dimethyl-5-deazaalloxazine), who proposed that it is driven by the change in the electron density on the nitrogen atoms of the molecule upon excitation [15]. Still, the question remains of the structure of hydrogen-bonded complexes in the ground and excited states, and of the specific atoms involved in their formation.

Published online: 23 November 2013

The aim of the present paper is to characterize spectroscopic and photophysical properties of 10-ethyl-5-deaza-isoalloxazine and its two structural analogues: 8-methyl-5-deazaalloxazine (8-Me-5-DAll) and 9-methyl-5-deazaalloxazine (9-Me-5-DAll). This work extends our previous studies concerning alloxazines to 5-deazaalloxazine (pyrimido[4,5-*b*]quinoline-2, 4(1*H*,3*H*)-dione) derivatives in which the N(5) atom is replaced by a carbon atom. Figure 1 presents the structures of the presently studied compounds. The difference between "alloxazinic" and "isoalloxazinic" structure of molecules lies in the position of their central double bonds. Molecules with "alloxazinic" structure have *s-cis*, while molecules with "isoalloxazinic" structure have *s-trans* double-bond configuration.

Besides spectroscopic and photophysical properties, we present results on the solvatochromism of the investigated compounds. Based on studies of solvent-dependent photophysical properties of these compounds, we discuss their ability to form solute-solvent hydrogen bonds in the ground and excited states. This is important for understanding their biological function, since hydrogen-bonding interaction is crucial for the appropriate description of the flavin derivatives belonging to LOV domains of the photoreceptors which respond to light, oxygen, or voltage [4].

Yagi and co-workers reported that hydrogen bonding at the heteroatoms of the isoalloxazine nucleus sequentially occurs, with increasing concentrations of the proton donor, first at N(l), then at O(2), O(4), and N(3)H, and finally at N(5) [16].

We also explore the processes occurring in singlet and triplet excited states in solution by means of theoretical studies using time-dependent density functional theory (TD-DFT). Earlier calculations that used time-dependent density theory (TD-DFT) show that all of the tested alloxazine derivatives have two pairs of closely-located n,π* and π, π* transitions in the lowest-energy part of the spectrum [17–22]. In most cases the states in a pair are isoenergetic, determining the photophysical properties of these compounds. However, to the best of our knowledge, there are no systematic experimental or theoretical studies of 5-deazaalloxazine derivatives, apart from theoretical calculations for some 5-deaza-isoalloxazines [23, 24].

Contrary to flavins, the lowest electronic transitions in 5-deazaflavins have a purely π,π* nature.

Experimental

Materials

Solvents: methanol (MeOH), ethanol (EtOH), 1-propanol (1-PrOH), 2-propanol (2-PrOH), 1-butanol (1-BuOH), 2-butanol (2-BuOH), pentanol (1-PeOH), hexanol (1-HeOH), acetonitrile (ACN), chloroform ($CHCl_3$), methylene chloride (CH_2Cl_2), 1,4-dioxane (1,4-Diox), ethyl acetate (AcOEt), acetone (Acet), dimethyl sulfoxide (DMSO) were all of spectroscopic or HPLC grade (Aldrich, Merck) and were dried before use with 3 Å or 4 Å molecular sieves from Fluka.

As the λ_{max} for the lowest-energy transitions did not vary much between solvents, it was determined with three replicates at a reduced scanning rate. The same precautions were taken for the emission λ_{max}, the latter was also determined for several λ_{exc} values.

10-ethyl-5-deaza-isoalloxazine (10-Et-5-DIAll), 8-methyl-5-deazaalloxazine (8-Me-5-DAll), and 9-methyl-5-deazaalloxazine (9-Me-5-DAll) were synthesized according to the procedures published by Yoneda et al. [25, 26] in a

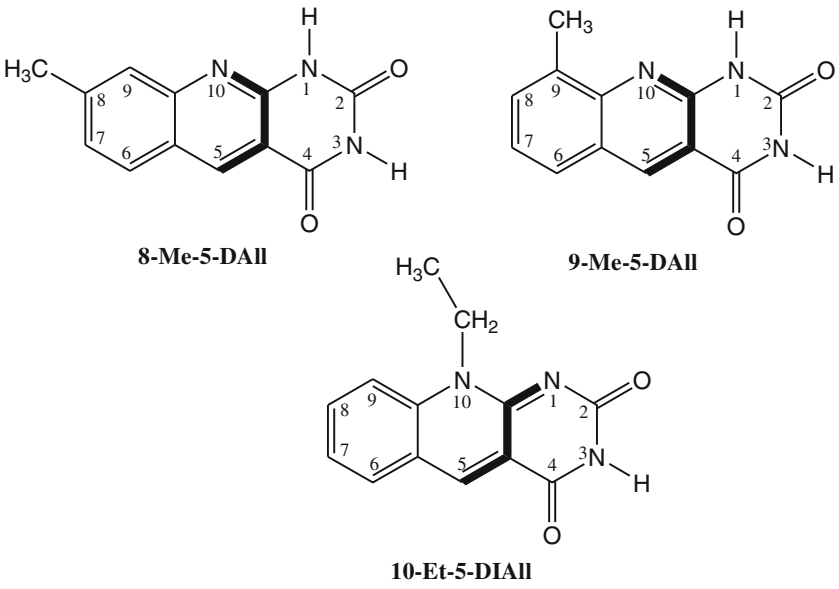

Fig. 1 Structures and abbreviations of the compounds studied and their corresponding atom numbering (8-Me-5-DAll: 8-methyl-5-deazaalloxazine; 9-Me-5-DAll: 9-methyl-5-deazaalloxazine; 10-Et-5-DIAll: 10-ethyl-5-deaza-isoalloxazine)

two-step synthesis. It should be pointed that the synthesis of 8-Me-5-DAll and 9-Me-5-DAll were not reported previously. First (step 1) we obtained the respective methyl substituted derivatives of 6-anilinouracils, next (step 2) we performed their cyclization using the Vilsmeier procedure. Water was triply distilled.

General Procedure for the Preparation of Pyrimido[4,5-b] Quinoline-2,4(1H,3H)-Diones

Step 1. [27]. To a stirred solution of aniline (3 ml) (*o*-methylaniline or *m*-methylaniline) were added hydrochloric acid (36 %, 6 mmol) and 6-aminouracil (6 mmol). The mixture was heated at 170–180 °C for 4–5 h. Diethyl ether was added after cooling and precipitated solids were collected by filtration. The corresponding 6-anilinouracils were obtained in 40–98 % yields.

Step 2. The appropriate 6-anilinouracil (1 g) was mixed with DMF (2 ml) and heated to 40 °C under stirring. Then phosphorus oxychloride (2.5 ml) was dropped into the mixture. The mixture was heated at 80 °C for 0.5 h. After cooling, excess DMF and $POCl_3$ were evaporated *in vacuo*. The solids were diluted with 5 % NH_4OH and then collected by suction filtration and washed with water. Crude products were recrystallized from glacial acetic acid.

Structures of the compounds studied were checked by ^1H and ^{13}C NMR and their purity was checked by thin-layer chromatography and elemental analysis.

(1) 8-Methylpyrimido[4,5-*b*]quinoline-2,4(1*H*,3*H*)-dione, (8-Me-5-DAll) (isolated yield 40 %; m.p. >350 °C with decomp. ^1H NMR (TFA-d): δ ppm: 2.81 (s, 3H, H_3C-C_8); 7.89 (d, 1H, H-7); 8.00 (s, 1H, H-9); 8.28 (d, 1H, H-6); 9.69 (s, 1H, H-C_5)); Anal. Calcd for $C_{12}H_9N_3O_2$: C, 63.44; H, 3.96; N, 18.50. Found: C, 63.51; H, 4.01; N, 18.29.

(2) 9-Methylpyrimido[4,5-*b*]quinoline-2,4(1*H*,3*H*)-dione, (9-Me-5-DAll) (isolated yield 35 %; m.p. 318 °C with decomp.); ^1H NMR (TFA-d): δ ppm: 2.91 (s, 3H, H_3C-C_9); 7.95 (t, 1H, H-7); 8.25 (d, 1H, H-8); 8.30 (d, 1H, H-6), 9.78 (s, 1H, C-5); Anal. Calcd for $C_{12}H_9N_3O_2$: C, 63.44; H, 3.96; N, 18.50. Found: C, 63.70; H, 3.89; N, 18.56.

(3) 10-ethylpyrimido[4,5-b]quinoline-2,4(3*H*,10*H*)-dione, (10-Et-5-DIAll) (isolated yield 74 %; m.p.>300 °C, lit. >300 °C [28]). ^1H NMR (TFA-d): δ ppm: 8.10 (m, 1H, H-Ar); 8.49 (m, 3H, H-Ar); 5.14 (m, 2H, -CH_2-), 1.89 (t, 3H, -CH_3), 9.78 (s, 1H, H-C_5); Anal. Calcd for $C_{13}H_{11}N_3O_2$: C, 64.73; H, 4.56; N, 17.43. Found: C, 64.75; H, 4.44; N, 17.40.

Methods

UV/Vis Measurements

All solutions were prepared on the same day as their absorbance, steady-state fluorescence, and fluorescence excitation spectra were recorded and time-resolved fluorescence measurements performed.

UV–vis absorption spectra were recorded on a Jobin Yvon-Spex Fluorolog 3–22 spectrofluorometer, using the option to measure absorption spectra; steady-state fluorescence excitation and emission spectra were also recorded on the same spectrofluorometer.

Fluorescence quantum yields were calculated relative to lumichrome as standard (φ_F=0.028) in acetonitrile [29]. We used the method described by Horiba Jobin-Yvon (gradient method) [30], with addition of simultaneous measurements of absorption and fluorescence on the same machine. Maximum absorption of all solutions was kept below 0.1. The estimated uncertainty of the fluorescence quantum yield is 20 %.

Lifetime Measurements

All fluorescence lifetime measurements were performed using the time-correlated single-photon counting (TCSPC) method. Decays were measured with an IBH Consultants (Glasgow, Scotland) System 5000 fluorescence lifetime spectrometer equipped with a NanoLED diode (λ_{exc} =374 nm, fwhm≈800 ps) from IBH as an excitation source. The instrument in this hardware configuration is capable of measuring lifetimes as short as 400 ps. Deconvolution of fluorescence decay curves was performed using Version 4 of the IBH Consultants software.

Laser Flash Photolysis

The setup for the nanosecond laser flash photolysis (LFP) experiments and its data acquisition system has been previously described in detail [31]. LFP experiments employed a pulsed Nd:YAG laser (355 nm, 4.5–5 mJ, 7–9 ns) for excitation. Transient decays were recorded at individual wavelengths by the step-scan method with a step distance of 10 nm in the range of 320 to 700 nm as the mean over 10 laser pulses. Samples for LFP were deoxygenated by bubbling high-purity argon for 15 min prior to the measurement. Experiments were performed in square fused-silica cells (1 cm).

All of the experiments were carried out at room temperature.

^1H NMR Measurements

The ^1H NMR spectra were recorded on a Varian Gemini 300 (300 MHz) Spectrometer in TFA-d solutions, the internal

standard was TMS. ^{1}H NMR spectra of the compounds studied were analyzed by comparison to those of similar compounds and by comparison to spectra calculated using the ACD/HNMR predictor [32].

TD-DFT Calculations

We used quantum-chemical calculations by means of the density-functional theory to obtain the information on the electronic structure and geometry of investigated derivatives of 5-deazaalloxazines. Recently, a relatively large number of iso- and alloxazines including monomethyl-substituted iso- and alloxazines, and di-, tri-, and tetramethyl-alloxazines, have been studied using similar TD-DFT calculations for singlet and triplet absorption spectra. Our own results [18, 20–23, 33, 34] and those published by Neiss et al.[17, 35] that used the TD-DFT approach for iso- and alloxazines demonstrated some very encouraging improvements as compared to previous semi-empirical and *ab initio* calculations [36, 37]. To allow direct comparison, the present calculations were made in exactly the same way as our earlier calculations of monomethyl-substituted derivatives of alloxazines [38]. Namely, the calculations were performed using the B3LYP functional [39] in conjunction with a modest 6-31+G(d) split-valence polarized basis set [40] and also using the polarizable continuum model (PCM) that employed B3LYP/6-31+G(d) level of calculation to include solvent effects. The B3LYP functional is one of the empirical hybrid density functional devised by Becke [39], which combines a fraction of the Hartree-Fock exchange functional with the correlation functional of Lee, Yang, and Parr [41]. The functional contains three parameters determined by fitting to selected properties of a large set of molecules. Oscillator strengths were calculated in the dipole length representation. Gaussian 09 *ab initio* program package was employed in calculations of excitation energies and oscillator strengths [42]. Atomic charges for the ground and the first excited singlet state of 8-Me-5DAll, 9-Me-5DAll and 10-Et-5-DIAll were calculated using the NBO population analysis.

Results and Discussion

Absorption and Emission Spectra

Absorption spectra of 8-Me-5-DAll, 9-Me-5-DAll and 10-Et-5-DIAll in selected organic solvents are presented in Fig. 2. Table 1 collects spectroscopic and photophysical data for the singlet states of 8-Me-5-DAll, 9-Me-5-DAll and 10-Et-5-DIAll, including absorption maxima (λ_1 and λ_2), emission maxima (λ_F), fluorescence lifetimes (τ_F), fluorescence quantum yields (ϕ_F) and the radiative (k_r) and the sum of non-radiative (Σk_{nr}) excited-state decay rate constants.

The two lowest-energy absorption maxima for 8-Me-5-DAll and for 9-Me-5-DAll are located between 349 nm to 362 nm (λ_1) and between 313 nm to 320 nm (λ_2) depending on solvent and derivative. For these compounds, we observe a blue shift of the first (λ_1) band in more polar alcohols, as compared to less polar alcohols. To compare, 10-Et-5-DIAll molecule needs less energy to excite. The absorption spectra of this compound include two characteristic bands at longer wavelengths with their maxima in the range from 395 nm to 401 nm (λ_1) and from 316 nm to 323 nm (λ_2), depending on the solvent. Our results indicate (see also DFT calculations results) that in both types of structures deazaalloxazine (8-Me-5-DAll and for 9-Me-5-DAll) and deazaisoalloxazine (10-Et-5-DIAll) the lowest-energy band has contribution from pure π,π^* transitions, contrary to alloxazines and flavins, for which at least two electronic transitions, mainly of the π,π^* and n,π^* type, contribute to the lowest-energy band, as has been reported by Kozioł already in sixties [43].

Figure 3 shows the emission spectra of 8-Me-5-DAll, 9-Me-5-DAll and 10-Et-5-DIAll in selected solvents. Typically we used the excitation wavelength λ_{exc}=370 nm for 10-Et-5-DIAll and λ_{exc}=350 nm for 8-Me-5-DAll and 9-Me-5-DAll, although the fluorescence spectrum was unaffected by the excitation wavelength. Note that the fluorescence excitation and absorption spectra agree well with each other in all of the solvents used. The emission maxima of 10-Et-5-DIAll appear in the range from 466 to 473 nm, red-shifted as compared to those of 8-Me-5-DAll and 9-Me-5-DAll in the same solvents. The emission maxima of 8-Me-5-DAll appeared between 401 and 411 nm, while those of 9-Me-5-DAll—from 416 to 425 nm, red-shifted as compared to 8-Me-5-DAll. The solvent polarity affects the exact position of the emission maxima, although the shifts are rather small. There is a red shift in polar solvents (alcohols) as compared to aprotic solvents for 8-Me-5-DAll and 9-Me-5-DAll, representing the 5-deazaalloxazine skeleton.

The radiative and non-radiative excited-state decay constants were calculated as $k_r=\phi_F / \tau_F$ and $\sum k_{nr}=(1-\phi_F) / \tau_F$ (see Table 1). In all cases the fluorescence decays are modeled well by single-exponential functions, as shown by the usual statistical criteria of "goodness-of-fit".

The values of the quantum yields of the presently investigated 5-deazalloxazines are an order of magnitude higher as compared to their "aza" analogues [38], while the quantum yields of isoalloxazines and 5-deaza-isoalloxazines are generally quite comparable [44]. Generally, the fluorescence quantum yields are rather high, compared to their "aza" analogs (i.e. alloxazines); however, the lower values we noted for 10-Et-5-DIAll.

For the investigated 5-deazaalloxazine derivatives, we see that the methyl group in position 8 causes a 2-fold increase in the fluorescence quantum yield, as compared to the impact of methyl group in position 9. Fluorescence quantum yields are

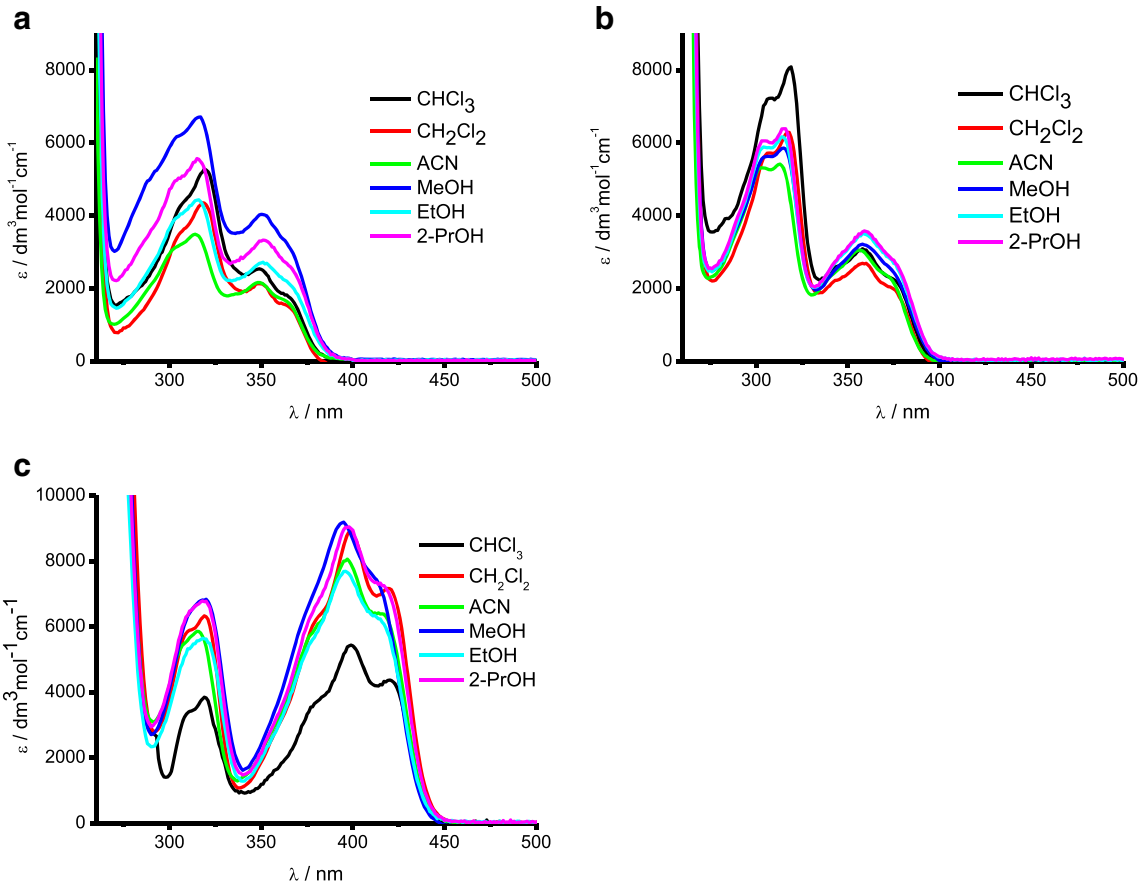

Fig. 2 Absorption spectra of **a** 8-Me-5-DAll, **b** 9-Me-5-DAll, and **c** 10-Et-5-DIAll; solvents indicated in each panel

affected by solvents, being higher in protic vs. aprotic solvents for both 8-Me-5-DAll and 9-Me-5-DAll, with an opposite tendency for 10-Et-5-DIAll.

The fluorescence lifetimes of 8-Me-5-DAll and 9-Me-5-DAll are an order of magnitude longer as compared to their "aza" analogues [38]. The fluorescence lifetimes of 5-deaza-isoalloxazines are about half of those for isoalloxazines [44, 45].

9-Me-5-DAll has the longest fluorescence lifetimes among the compounds presently studied. On the other hand, protic solvents (alcohols) enhance fluorescence lifetimes for both 5-alloxazine derivatives, more so for 9-Me-5-DAll and less for 8-Me-5-DAll. This shows that the location of the methyl group on the alloxazinic skeleton significantly affects the fluorescence lifetime (see Table 1 for details).

The calculated radiative and non-radiative decay constants (Table 1) show that the non-radiative constants are from two—to ten-fold higher than the radiative constants.

Solvatochromic Studies

To check the influence of solvent parameters on spectral and photophysical properties of monomethyl derivatives of 5-deazaalloxazine and 10-ethyl-5-deaza-isoalloxazine, we used the Δf solvent polarity scale and the four-parameter Catalán scale [46].

The Δf solvent polarity scale takes into account the general solvent effects, including nonspecific interactions between solute and solvent, of electrostatic and dispersive origin, arising from solvent acting as a dielectric continuum, and is based on the Onsager's reaction field theory with the general form of Lippert-Mataga solvent polarity function [47, 48]:

$$\Delta f = \frac{\varepsilon - 1}{2\varepsilon + 1} - \frac{n^2 - 1}{2n^2 + 1} \quad (1)$$

This function is dependent on the relative permittivity ε (formerly—the dielectric constant) and the refractive index, describing non-specific solute-solvent interactions. All of the numeric data required to calculate Δf were taken from Reynolds et al. [49].

The dependence of the absorption maxima on the orientational polarizability Δf for 8-Me-5-DAll, 9-Me-5-DAll and 10-Et-5-DIAll in selected solvents is shown in Figure 1s, and the dependence of the emission maxima is shown in Figure 2s, both in Supporting Information.

From the results given in Figures 1s and 2s we see that the solvatochromic properties of the investigated compounds do

Table 1 Spectroscopic and photophysical data for the singlet states of 8-Me-5-DAll, 9-Me-5-DAll and 10-Et-5-DIAll

Solvent	Compound	λ_1/nm	λ_2/nm	λ_F/nm	$\Delta\nu$ / cm^{-1}	ϕ_F	τ_F /ns	k_r /10^8 s^{-1}	Σk_{nr} /10^8 s^{-1}
1,4-Diox	8-Me-5-DAll	350	314	404	3737	0.12	3.20	0.38	2.75
	9-Me-5-DAll	356	313	416	4051	0.22	6.16	0.36	1.27
	10-Et-5-DIAll	399	317	473	3920	0.12	4.71	0.25	1.87
$CHCl_3$	8-Me-5-DAll	349	320	407	4083	0.13	2.86	0.45	3.04
	9-Me-5-DAll	358	319	417	3854	0.29	8.63	0.34	0.82
	10-Et-5-DIAll	399	319	468	3700	0.09	3.31	0.27	2.74
CH_2Cl_2	8-Me-5-DAll	349	319	403	3839	0.11	2.93	0.38	3.04
	9-Me-5-DAll	358	317	417	3952	0.25	8.38	0.29	0.89
	10-Et-5-DIAll	398	320	468	3600	0.11	3.44	0.32	2.59
AcOEt	8-Me-5-DAll	351	313	401	3552	0.09	2.96	0.31	3.07
	9-Me-5-DAll	356	314	416	4051	0.17	5.35	0.32	1.55
	10-Et-5-DIAll	401	316	470	3720	0.07	4.59	0.15	2.03
DMSO	8-Me-5-DAll	355	315	409	3719	0.16	2.85	0.56	2.94
	9-Me-5-DAll	362	316	419	3834	0.22	7.07	0.31	1.10
	10-Et-5-DIAll	397	323	469	3740	0.02	2.09	0.10	4.69
Acet	8-Me-5-DAll	352	-	404	3656	0.12	3.10	0.39	2.84
	9-Me-5-DAll	358	-	416	3894	0.23	5.99	0.38	1.29
ACN	8-Me-5-DAll	349	315	402	3777	0.14	3.58	0.39	2.40
	9-Me-5-DAll	356	314	416	3952	0.25	8.06	0.31	0.93
	10-Et-5-DIAll	397	317	467	3650	0.16	4.05	0.40	2.07
1-HeOH	8-Me-5-DAll	353	317	410	3938	0.18	4.19	0.43	1.96
	9-Me-5-DAll	361	317	423	4060	0.30	11.2	0.27	0.63
	10-Et-5-DIAll	398	320	471	3890	0.07	3.56	0.20	2.61
1-PeOH	8-Me-5-DAll	353	318	409	3878	0.17	4.18	0.41	1.99
	9-Me-5-DAll	362	317	422	3927	0.32	11.2	0.29	0.61
	10-Et-5-DIAll	397	319	466	3730	0.06	3.55	0.17	2.65
2-BuOH	8-Me-5-DAll	354	313	411	3917	0.19	4.25	0.48	1.91
	9-Me-5-DAll	362	320	423	3983	0.38	12.1	0.31	0.51
	10-Et-5-DIAll	397	319	466	3730	0.09	3.49	0.26	2.61
1-BuOH	8-Me-5-DAll	353	317	410	4018	0.18	4.19	0.43	1.96
	9-Me-5-DAll	361	317	425	4171	0.41	13.7	0.30	0.43
	10-Et-5-DIAll	397	319	470	3790	0.09	3.52	0.26	2.59
1-PrOH	8-Me-5-DAll	353	318	408	3818	0.17	4.21	0.40	1.97
	9-Me-5-DAll	360	317	423	4137	0.31	11.3	0.27	0.61
	10-Et-5-DIAll	397	323	466	3670	0.08	3.51	0.23	2.62
2-PrOH	8-Me-5-DAll	352	317	409	3959	0.19	4.03	0.47	2.00
	9-Me-5-DAll	359	316	421	4024	0.36	10.32	0.35	0.62
	10-Et-5-DIAll	398	320	468	3700	0.07	3.51	0.20	2.65
EtOH	8-Me-5-DAll	352	316	409	3959	0.16	4.25	0.38	1.98
	9-Me-5-DAll	358	314	423	4137	0.31	11.04	0.28	0.63
	10-Et-5-DIAll	396	318	468	3900	0.08	3.54	0.23	2.60
MeOH	8-Me-5-DAll	351	316	410	4099	0.16	4.58	0.35	1.83
	9-Me-5-DAll	358	315	425	4380	0.31	12.6	0.25	0.55
	10-Et-5-DIAll	395	320	466	3790	0.09	3.58	0.25	2.54

[a] λ_1, λ_2 are the positions of the two lowest-energy bands in the absorption spectra, λ_F the fluorescence emission maximum, ϕ_F the fluorescence quantum yield, τ_F the fluorescence lifetime, $\Delta\nu$—Stoke's shift, k_r the radiative rate constant and Σk_{nr} the sum of non-radiative rate constants

not show any regular solvatochromic tendency in the function of solvent polarity parameter Δf in all solvents used. However, taking protic solvents separately, we found a linear correlation between the absorption maxima and Δf, for

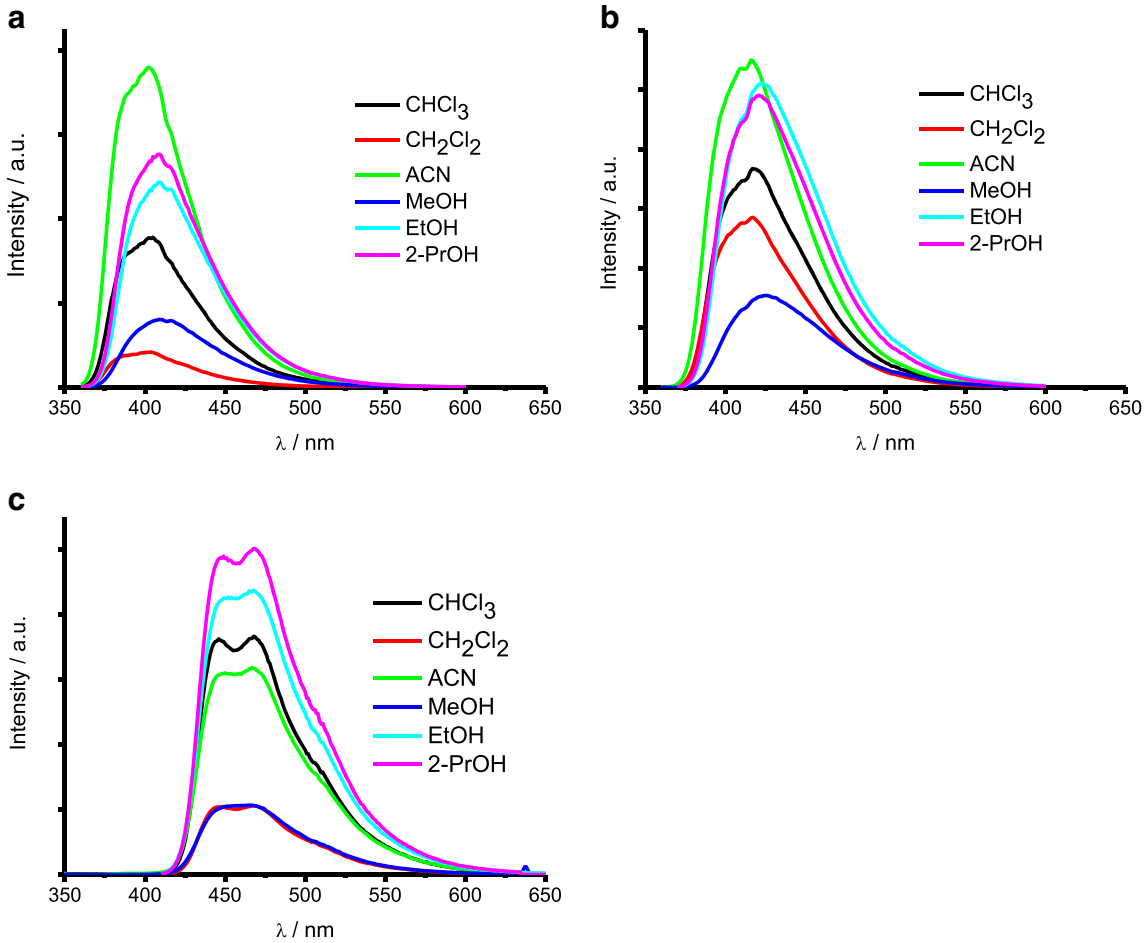

Fig. 3 Emission spectra of **a** 8-Me-5-DAll, **b** 9-Me-5-DAll, and **c** 10-Et-5-DIAll; solvents indicated in each panel. Here, λ_{exc}=350 nm for 8-Me-5-DAll and 9-Me-5-DAll and 370 nm for 10-Et-5-DIAll

example the linear correlation coefficient is R=0.89 for 9-Me-5-DAll, and R=0.77 for 8-Me-5-DAll. Mitra and Mayon [50] obtained similar results for lumichrome (7, 8-dimethylalloxazine), investigating its photophysical properties in different solvents. Taking in account such poor correlations we did not try calculating the dipole moments in the excited state of the investigated compounds, using solvatochromic study. These results may also suggest that the dipole moments of these compounds may be quite similar in the S_0 and S_1 states. Indeed it was confirmed by theoretical calculations discussed below. The same has already been noted for 5-DAll and 7,8-dimethyl-5-deazaalloxazine [14]. The correlation between the emission maxima vs. Δf is unacceptable for 8-Me-5-DAll and 9-Me-5-DAll in both protic and aprotic solvents; however, for 10-Et-5-DIAll we have an acceptable correlation coefficient (R=0.75) of the emission maxima in aprotic solvents. These results suggest also that for the target compounds specific solvent-solute interactions may have importance both in the ground state and first excited state. Such interactions are indeed confirmed by using the Catalán scale (see below).

Thus, we used multilinear correlation for a detailed analysis of the solvent properties that affect the spectroscopic and photophysical properties of the studied compounds. The respective equation takes in account four different solvent properties:

$$A = A_0 + a_{SP}SP + b_{SdP}SdP + c_{SA}SA + d_{SB}SB \quad (2)$$

Here, A_0 is the statistical quantity corresponding to the value of the property in the gas phase; SA, SB, SP, and SdP represent independent solvent parameters and a_{SP}, b_{SdP}, c_{SA}, and d_{SB} are the regression coefficients describing the sensitivity of the property A to the different solute-solvent interaction mechanisms [46].

This scale is based on specific and general scales, using four parameters (SA—solvent acidity, SB—solvent basicity, SdP—solvent dipolarity and SP—solvent polarizability scales), as has been recently proposed by Catalán [46], where SA and SB describe specific solvent-solute interactions, such as hydrogen bonding, and SdP and SP are responsible for the non-specific effects.

The four-parameter Catalán scale, contrary to a prior three-parameter scale [51], uses separate dipolarity and polarizability parameters, discriminating their contributions to the photophysical properties of the compounds investigated. Thus, we expected a better description of the solvent effects on the absorption and emission energies. Thus, multilinear regressions for 8-Me-5-DAll, 9-Me-5-DAll and 10-Et-5-DIAll were calculated and the estimated regression coefficients—a_{SP}, b_{SdP}, c_{SA}, and d_{SB} are presented in Table 2 along with the correlation coefficients R.

The best correlation coefficient (R=0.94) was obtained for the absorption maxima of 8-Me-5-DAll; these values are worse for 9-Me-5-DAll (R=0.88) and for10-Et-5-DIAll (R=0.82). We note some similarities for 8-Me-5-DAll and 9-Me-5-DAll, as their absorption maxima depend mainly on the solvent polarizability (SP), the a_{SP} coefficients being negative for both compounds. Thus, increased solvent polarizability destabilizes these compounds in their ground state. Interestingly, the influence of the solvent basicity on the absorption maxima of 9-Me-5-DAll is greater than that of the solvent acidity. In the extreme case of 8-Me-5-DAll, the effect of solvent acidity on the absorption maxima is negligible compared to that of solvent basicity.

All of the studied compounds can act both as a donor and as an acceptor of hydrogen bonds. The hydrogen bonds in protic solvents may form between hydrogen of the hydroxyl group in alcohols and N(10)—for 8-Me-5-DAll and 9-Me-5-DAll, or N(1)—for 10-Et-5-DIAll, and/or C=O groups of these compounds, acting as acceptors. Additionally, the same compounds can act as hydrogen donors, because of presence of N(3)-H and/or N(1)-H groups. Analysis using the four-parameter Catalán scale indicates that such hydrogen bonds where N(3)-H (or N(1)-H) acting as hydrogen-bond donors are possible in 8-Me-5-DAll, and to a less extent in 9-Me-5-DAll. We also conclude that 8-Me-5-DAll does not act as the hydrogen-bonds acceptor in the ground state. Thus N(10) and C=O groups in 8-Me-5-DAll are not involved in hydrogen bonds in the ground state, because c_{SA}=0. Contrary to that, 9-Me-5-DAll can act as both hydrogen-bond donor and acceptor in the ground state. Still, the absorption maxima are more affected by the hydrogen-bond donating ability and less by the hydrogen bond accepting ability of this molecule.

Interestingly, the solvent basicity is the main factor that affects the absorption maxima for 10-Et-5-DIAll; however the correlation is poorer but still acceptable. We suggest that the hydrogen bond mainly involves the N(1) atom, this being the main protonation site in 10-Et-5-DIAll (pK_a=1.64), with the highest electron density among the heteroatoms that may be hydrogen bond acceptors. Data and discussion on the calculated electron densities at atoms in the ground and in the excited state of the investigated molecules are presented in the following section.

Different results are observed for the emission maxima of 8-Me-5-DAll and 9-Me-5-DAll, these being mainly dependent on polarizability and acidity of solvents. The SP and SA parameters provide a good description of the emission maxima for these compounds, with high correlation coefficients (R=0.92 and R=0.98, respectively). However, the solvent acidity has the highest impact on the emission maxima of 9-Me-5-DAll, while the polarizability has the highest impact on the emission maxima of 8-Me-5-DAll.

The data of Table 2 demonstrate that 8-Me-5-DAll acts as hydrogen bond donor in the ground state and hydrogen bond acceptor in the excited state. According to our previous studies [52, 53] and literature [50], we suggest that hydrogen bonds in

Table 2 Results of the regression calculations: the value of the property in the gas phase-A_0 and the estimated coefficients: a_{SP}, b_{SdP}, c_{SA} and d_{SB}, see Eq. (2), standard errors and correlation coefficients (R) for the multilinear regression analysis of the absorption maxima (ν_{abs}) and emission maxima (ν_{em})

Property	A_0	a_{SP}	b_{SdP}	c_{SA}	d_{SB}	R
8-Me-5-DAll						
ν_{abs} / cm^{-1}	29544±242	−938±299	−175±89	59±116	−609±80	0.94
ν_{abs} / cm^{-1}	29579±220	−997±266	−169±85	–	−587±65	0.94
ν_{em} / cm^{-1}	26047±379	−1592±469	−49±140	−887±182	−275±124	0.92
ν_{em} / cm^{-1}	25992±332	−1570±446	–	−897±173	−265±116	0.92
9-Me-5-DAll						
ν_{abs} / cm^{-1}	29602±347	−1807±420	−191±130	−234±89	−534±86	0.89
ν_{abs} / cm^{-1}	29391±331	−1724±437	–	−270±90	−497±87	0.88
ν_{em} / cm^{-1}	24474±200	−544±247	16±74	−942±96	−187±66	0.98
ν_{em} / cm^{-1}	24492±175	−551±234	–	−939±91	−189±61	0.98
10-Et-5-DIAll						
ν_{abs} / cm^{-1}	24770±277	240±354	210±104	423±146	−51±88	0.84
ν_{abs} / cm^{-1}	24918±69	–	227±95	324±92	–	0.82
ν_{em} / cm^{-1}	21316±86	−204±450	245±132	212±186	−74±111	0.71
ν_{em} / cm^{-1}	21122±86	–	266±120	189±117	–	0.68

the excited state form mainly between protic solvents and the N(10) atom and that C=O groups are not involved. This conclusion is also valid for 9-Me-5-DAll, however the situation here is slightly different. The data of Table 2 indicate that the N(10)···H-O intermolecular hydrogen bond we postulated is significantly stronger in the electronic excited state compared to the ground state. This follows from the fact that the c_{SA} coefficient is higher in the excited as compared to the ground state. In contrast, hydrogen bonds between the donating N-H groups and solvents are weaker in the excited as compared to the ground state.

We can not correlate the emission maxima of 10-Et-5-DIsoAll with the solvent parameters, as the calculated R~ 0.70 value is quite poor. This indicates that solvents have almost no effect on the emission maxima. We believe that the main reason for that is the ethyl substituent at N(10), which excludes hydrogen bond between N(10) and hydrogen-donating solvents.

Catalán scale does describe sufficiently well neither the fluorescence quantum yields (ϕ_F), nor fluorescence lifetimes (τ_F), radiative k_r nor non-radiative (Σk_{nr}) rate constants of the investigated compounds (data not presented). The solvent-dependent coefficients (a_{SP}, b_{SdP}, c_{SA}, and d_{SB}) do not reflect the real change in these values and their individual errors are quite high.

Transient Absorption Spectra

Figure 4 shows transient absorption spectra of 8-Me-5-DAll, 9-Me-5-DAll and 10-Et-5-DIAll in acetonitrile. Transient absorption spectra were recorded upon laser excitation at 355 nm. Note that acetonitrile as a polar but aprotic solvent is not able to create hydrogen bonds with dissolved molecules as a hydrogen donor. To the best of our knowledge, there are no published experimental transient absorption data for the 5-deazaalloxazines.

According to Fig. 4b and c negative absorbance (bleaching) appears at 370 nm (9-Me-5-DAll) and at 400 nm (10-Et-5-DIAll) because of ground-state depletion upon excitation. No negative absorbance is observed for 8-Me-5-DAll in the spectral range probed (Fig. 4a). 5-Deazalloxazine derivatives produce spectra that are similar to those recorded for alloxazines, although bathochromically shifted by about 100 nm [18, 34, 54, 55]. The global analysis of the experimental triplet state decays indicates the presence of only one

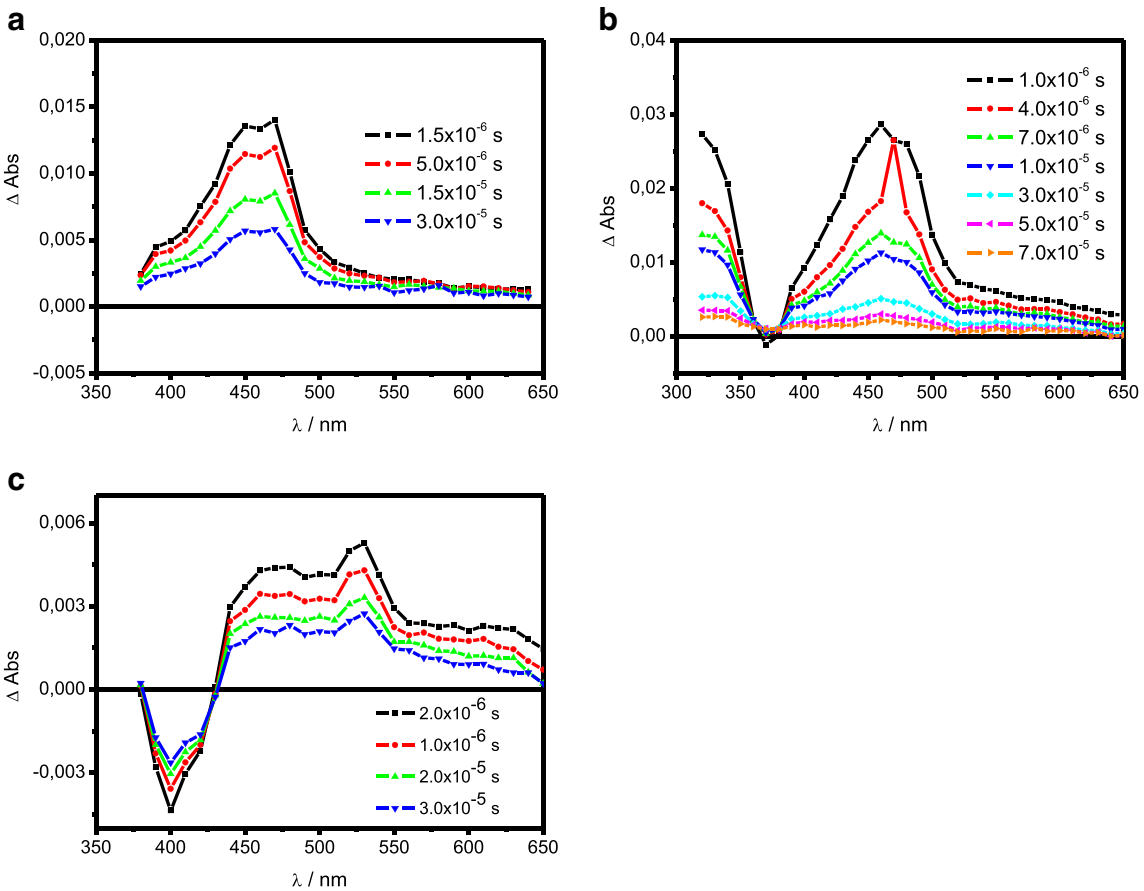

Fig. 4 Experimental transient absorption spectra of 5-deazaalloxazine derivatives: **a** 8-Me-5-DAll, **b** 9-Me-5-DAll, and **c** 10-Et-5-DIAll, in acetonitrile, excited at 355 nm, using OD_{355}=0.15, 1.5 mJ/pulse, l=1 cm

species, with the triplet lifetime being in the microsecond time range.

There are two strong maxima for 8-Me-5-DAll, one at about 450 nm (22 200 cm^{-1}) and 470 nm (21 280 cm^{-1}) and smaller one at about 530 nm (18 867 cm^{-1}). Three maxima appear for 9-Me-5-DAll, at about 310 nm (32 258 cm^{-1}), 460 nm (21 700 cm^{-1}) and 480 nm (20 800 cm^{-1}) respectively. There is a strong negative absorbance for 10-Et-5-DIAll at 400 nm (25 000 cm^{-1}), two positive maxima located at about 480 nm (20 800 cm^{-1}) and 530 nm (18 867 cm^{-1}). The two lowest-energy absorption bands of 10-Et-5-DIAll are bathochromically shifted with respect to those of their "aza" analogs [45, 56–59].

Singlet and Triplet States: Theoretical Approach

We used the optimized ground state geometry for calculations that predicted the lowest-energy singlet-singlet $S_0 \rightarrow S_i$ transitions as well as spin-forbidden $S_0 \rightarrow T_i$ transitions, whereas $T_1 \rightarrow T_i$ excitation energies and transition intensities were determined for the optimized geometry of the lowest triplet state (T_1), using the unrestricted method suitable for open shell systems. To verify the type of the minimum located, the geometry optimization was followed by the vibrational frequency calculations, which revealed no imaginary frequencies.

Figure 5 shows the calculated lowest-energy singlet-singlet transitions of 8-Me-5-DAll, 9-Me-5-DAll and 10-Et-5-DIAll, compared to their experimental spectra in 1,4-dioxane. The predicted energies of the lowest singlet-singlet transitions with calculated dipole moments in S_0 and S_1 states for 8-Me-5-DAll, 9-Me-5-DAll and 10-Et-5-DIAll are listed in Table 3.

It should be pointed that the predicted value of the $S_0 \rightarrow S_1$ transition energy in the gas phase determined according to the Catalán scale for 8-Me-5-DAll, A_0=29579 cm^{-1} (Table 2) agrees well with value calculated, using TD-DFT method,

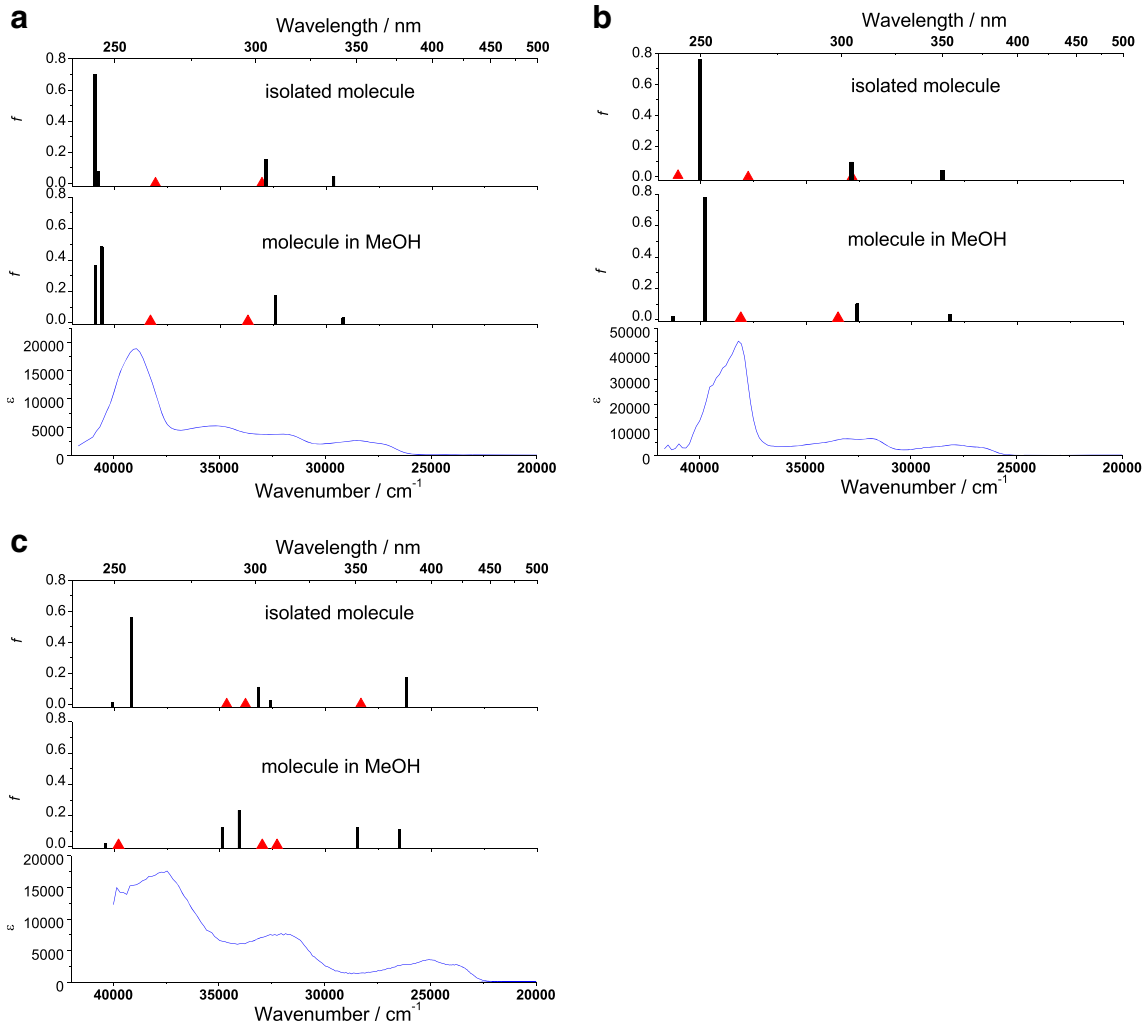

Fig. 5 Absorption spectra of 8-Me-5-DAll (**a**), 9-Me-5-DAll (**b**), and 10-Et-5-DIAll (**c**) in 1,4-dioxan. Predicted transition energies and oscillator strengths *f* are indicated by *solid vertical lines* (for isolated molecule—top panels, and MeOH solutions—middle panels). The (prohibited) transitions involving the n, π* singlet states are marked by *red triangles*

Table 3 The lowest predicted [B3LYP/6-31+G(d)] singlet excitation energies for isolated molecule, starting from the ground state of 8-Me-5-DAll, 9-Me-5-DAll, 10-Et-5-DIAll with the corresponding oscillator strengths, f. The highest occupied and the lowest unoccupied MOs are represented by the respective orbital numbers

$S_0 \rightarrow S_i$	8-Me-5-DAll			9-Me-5-DAll			10-Et-5-DIAll		
	$E \times 10^{-3}$ / cm^{-1}	f	μ / D	$E \times 10^{-3}$ / cm^{-1}	f	μ / D	$E \times 10^{-3}$ / cm^{-1}	f	μ / D
S_0	Ground state		4.7			4.0			7.8
$\rightarrow S_1$	29.6	0.044	4.6	28.6	0.0396	3.9	26.2	0.1701	10.2
	59→60 (62 %)			58→61 (13 %)			61→65 (10 %)		
	58→61 (17 %)			59→60 (66 %)			63→64 (65 %)		
$\rightarrow S_2$	32.8	0.152	–	32.8[a]	0.0005	–	28.3[a]	0.0017	–
	58→60 (61 %)			57→60 (68 %)			58→64 (11 %)		
	59→61 (28 %)						62→64 (68 %)		
$\rightarrow S_3$	33.0[a]	0	–	32.9	0.0963	–	32.6	0.0230	–
	57→60 (68 %)			58→60 (60 %)			59→64 (54 %)		
				59→61 (−32 %)			63→65 (17 %)		
$\rightarrow S_4$	38.1[a]	0	-	37.7[a]	0.0002	–	33.2	0.0401	–
$\rightarrow S_5$	40.8	0.076	–	40.1	0.7588	–	33.8[a]	0.0008	–
$\rightarrow S_6$	40.9	0.699	–	41.1[a]	0.009	–	34.7[a]	0.0133	–
$\rightarrow S_7$	41.8[a]	0	–	41.8[a]	0	–	39.2	0.5632	–
$\rightarrow S_8$	42.7	0.253	–	42.6[a]	0.0003	–	40.1	0.0103	–
$\rightarrow S_9$	42.8[a]	0	–	42.7	0.1345	–	40.5	0.1642	–
$\rightarrow S_{10}$	44.7	0.342	–	45.1	0.1345	–	41.1	0.0112	–
$\rightarrow S_{11}$	46.4	0.137	–	45.9	0.0783	–	43.5[a]	0.0022	–
$\rightarrow S_{12}$	47.1[a]	0	–	46.7[a]	0.0012	–	44.8[a]	0.0035	–
$\rightarrow S_{13}$	47.7	0.105	–	47.1[a]	0	–	45.6[a]	0.0021	–
$\rightarrow S_{14}$	47.9[a]	0	–			–	46.1	0.3654	–
$\rightarrow S_{15}$	49.1	0.213	–			–	46.4	0.0540	–

[a] n,π^* transition, otherwise π,π^*

for isolated molecule, E=29600 cm^{-1} (Table 3). Also the $S_0 \rightarrow S_1$ transition energy in the gas phase for 9-Me-5-DAll, A_0=29391 cm^{-1} (Table 2) agrees with value calculated for isolated molecule, E=28600 cm^{-1} (Table 3). The difference becomes still larger for 10-Et-5-DIAll, achieving 1280 cm^{-1}, the respective values being 24918 cm^{-1}, Table 2 and 26200 cm^{-1}, Table 3. The A_0 values in the gas phase for the lowest-energy transitions, calculated from the experimental data, according to the Catalán regression method are valuable because usually there are no experimental gas-phase spectra of the investigated compounds available for comparison. The TD-DFT calculations provide a value that agrees well to that determined experimentally (especially for 8-Me-5-DAll). It means that the theory describe well the experimental data.

The calculated dipole moment for 10-Et-5-DIAll in the ground state is highest between other compounds (μ=7.8 D). These dipole moments for 8-Me-5-DAll and for 9-Me-5-DAll are similar (μ=4.7 D and 4.0 D, respectively). They diminish slightly in their S_1 states (μ=4.6 D and 3.9 D, respectively) for the latest compounds. But the dipole moment for 10-Et-5-DIAll increases in the S_1 state (μ=10.8 D).

We previously found that in a series of alloxazine derivatives each of the two lowest-energy π,π^* transitions are accompanied by a closely-located n,π^* transition, which has a very similar energy. It is interesting that the presently investigated 5-deazaalloxazine derivatives are an exception, because here the lowest-energy π,π^* transitions are not accompanied by closely-located n,π^* transition (8-Me-5-DAll and 9-Me-5-DAll) or additionally have a large energy gap between the π, π^* states (10-Et-5-DIAll, Fig. 5).

Note that in 8-Me-5-DAll both $S_0 \rightarrow S_1$ and $S_0 \rightarrow S_2$ transitions have pure π,π^* character. The energy gap between the two lowest singlet excited states is $|E_{\pi,\pi^*} - E_{\pi,\pi^*}|$=3200 cm^{-1}. The energy separation of the two first singlet states in 9-Me-5-DAll is $|E_{n,\pi^*} - E_{\pi,\pi^*}|$=4200 cm^{-1} and 2100 cm^{-1} in 10-Et-5-DIAll. Note that the values of the fluorescence quantum yield are an order of magnitude higher than those of the respective alloxazine analogues in the same solvents. This is a consequence of their lowest energy transitions having pure π,π^* character.

Additionally, Table 4 lists the predicted $S_0 \rightarrow S_i$ excitation energies calculated taking into account the solvent (methanol)

Table 4 The lowest predicted [B3LYP/6-31+G(d)] singlet excitation energies starting from the ground state calculated taking into account the solvent (methanol) by virtue of the polarizable continuum model of 8-Me-5-DAll, 9-Me-5-DAll, 10-Et-5-DIAll with the corresponding oscillator strengths, *f*. The highest occupied and the lowest unoccupied MOs are represented by the respective orbital numbers

$S_0 \rightarrow S_i$	8-Me-5-DAll		9-Me-5-DAll		10-Et-5-DIAll	
	$E \times 10^{-3}$ / cm^{-1}	*f*	$E \times 10^{-3}$ / cm^{-1}	*F*	$E \times 10^{-3}$ / cm^{-1}	*f*
$\rightarrow S_1$	29.2	0.0321	28.2	0.0345	26.5	0.1121
	58→61 (13 %)		58→61 (10 %)		61→65 (12 %)	
	59→60 (69 %)		59→60 (69 %)		63→64 (67 %)	
$\rightarrow S_2$	32.4	0.1755	32.6	0.1016	28.5	0.1236
	58→60 (64 %)		58→60 (62 %)		58→64 (13 %)	
	59→61 (−27 %)		59→61 (−31 %)		62→64 (66 %)	
$\rightarrow S_3$	33.7[a]	0.0005	33.5[a]	0.0005	32.3[a]	0.0001
	57→60 (69 %)		57→60 (70 %)		59→64 (51 %)	
					63→65 (16 %)	
$\rightarrow S_4$	38.3[a]	0.0002	38.1[a]	0.0001	33.0[a]	0.0005
$\rightarrow S_5$	40.6	0.4850	39.8	0.7823	34.1	0.2342
$\rightarrow S_6$	40.9	0.3664	41.3	0.0224	34.9	0.1232
$\rightarrow S_7$	42.6[a]	0.0001	42.5[a]	0.0001	39.8[a]	0.0002
$\rightarrow S_8$	43.3	0.2080	43.3	0.1091	40.4	0.0232
$\rightarrow S_9$	43.4[a]	0.0001	43.5[a]	0	41.1	0.1122
$\rightarrow S_{10}$	44.2	0.3096	44.7	0.2082	41.9	0.0987
$\rightarrow S_{11}$	45.9	0.0659	45.4	0.1432	43.9[a]	0.0002
$\rightarrow S_{12}$	47.5	0.1146	47.1[a]	0.0013	45.1	0.0234
$\rightarrow S_{13}$	47.9[a]	0	47.9	0.1997	46.0[a]	0
$\rightarrow S_{14}$	48.6[a]	0.0002	48.1[a]	0	46.3[a]	0.0003
$\rightarrow S_{15}$	48.6	0.2723	48.4	0.1786	46.5	0.1762

[a] *n*,π* transition, otherwise π,π*

by virtue of the polarizable continuum model (PCM). In fact, comparison between the data obtained for an isolated molecule and from PCM shows that the $S_0 \rightarrow S_1$ transition has π, π* character in each case (Tables 3 and 4). The energy differences of about 400 cm^{-1} were calculated between isolated molecules and molecules in methanol for the $S_0 \rightarrow S_1$ transition in 8-Me-5-DAll and 9-Me-5-DAll. The energies of these transitions in gase phase are higher than the same energies calculated for methanol. At the same time, we noted a reverse trend for 10-Et-5-DIAll. Additionally, calculations indicate for 8-Me-5-DAll and 9-Me-5-DAll that the S_2 and S_3 states are isoenergetic in the gas phase, whereas PCA calculations indicate that solvent causes the respective two transitions to appear separately, $S_0 \rightarrow S_2$ and $S_0 \rightarrow S_3$ (see Fig. 5a and b). The situation is different for 10-Et-5-DIAll, here gas-phase calculations indicate that the $S_0 \rightarrow S_2$ transition has a pure n,π* character, in contrast to the results of PCA analysis that indicate a pure π,π* character. Both in gas phase and modeled solvent environment (PCA analysis) the $S_0 \rightarrow S_1$ transition is well separated and has π,π* character.

The lowest predicted energies of singlet-triplet transitions for 8-Me-5-DAll, 9-Me-5-DAll and 10-Et-5-DIAll and the lowest predicted energies of their triplet-triplet transitions are presented in Tables 5 and 6, respectively.

T-T excitation energies and oscillator strengths were determined for the optimized geometry of the lowest triplet state (T_1). The theoretical triplet-triplet transitions are blue-shifted compared to the experimental transient absorption spectra. This is more pronounced for 10-Et-5-DIAll than for 8-Me-5-DAll or 9-Me-5-DAll. This is also due to the fact that the theoretical calculations are made for gas-phase molecules, whereas the experimental spectra are recorded in acetonitrile solutions. The detectable theoretically predicted transitions in 8-Me-5-DAll are located at about 19 800, 23 300, 25 800, and 30 800 cm^{-1}. The detectable transitions for 9-Me-5-DAll appear at 20 300, 23 200, 25 900, and 30 700 cm^{-1}; and those

Table 5 The lowest predicted (B3LYP /6-31+G(d)) $S_0 \rightarrow T_i$ excitation energies of 8-Me-5-DAll, 9-Me-5-DAll, and 10-Et-5-DIAll with their corresponding oscillator strengths, *f*

$S_0 \rightarrow T_i$	8-Me-5-DAll		9-Me-5-DAll		10-Et-5-DIAll	
	$E \times 10^{-3}$/ cm^{-1}	*F*	$E \times 10^{-3}$/ cm^{-1}	*F*	$E \times 10^{-3}$ / cm^{-1}	*f*
$\rightarrow T_1$	21.8	0	20.8	0	19.5	0
$\rightarrow T_2$	25.5	0	25.9	0	23.8	0
$\rightarrow T_3$	30.8	0	30.1	0	26.9	0
$\rightarrow T_4$	30.9	0	30.6	0	29.2	0
$\rightarrow T_5$	33.7	0	33.2	0	30.3	0
$\rightarrow T_6$	35.1	0	34.9	0	31.6	0
$\rightarrow T_7$	35.7	0	36.1	0	32.1	0

Table 6 The lowest predicted (uB3LYP /6-31+G(d)) $T_1 \rightarrow T_i$ excitation energies of 8-Me-5-DAll, 9-Me-5-DAll, and 10-Et-5-DIAll with their corresponding oscillator strengths, *f*

$T_1 \rightarrow T_i$	8-Me-5-DAll		9-Me-5-DAll		10-Et-5-DIAll	
	$E \times 10^{-3}$ / cm^{-1}	*f*	$E \times 10^{-3}$ / cm^{-1}	*F*	$E \times 10^{-3}$ / cm^{-1}	*f*
$\rightarrow T_2$	8.2	0.004	8.8	0.0041	5.8	0.0068
$\rightarrow T_3$	11.2	0	12.6	0.0067	8.9	0
$\rightarrow T_4$	12.8	0.004	12.8	0.0001	12.5	0.0074
$\rightarrow T_5$	15.4	0.001	15.6	0.0011	13.1	0.0003
$\rightarrow T_6$	16.5	0	17.3	0.0001	13.7	0.0039
$\rightarrow T_7$	18.5	0	19.4	0.0011	14.0	0
$\rightarrow T_8$	19.8	0.020	20.3	0.0118	17.0	0.0486
$\rightarrow T_9$	21.3	0	22.2	0	19.4	0.0057
$\rightarrow T_{10}$	23.3	0.195	23.2	0.2041	20.7	0.1215
$\rightarrow T_{11}$	25.8	0.024	25.9	0.0236	24.9	0.1551
$\rightarrow T_{12}$	27.8	0	26.9	0.0016	27.0	0.0016
$\rightarrow T_{13}$	29.8	0	28.5	0	28.3	0.0679
$\rightarrow T_{14}$	30.8	0.024	30.7	0.0231	29.7	0.0009
$\rightarrow T_{15}$	31.5	0	30.9	0.0007	30.3	0.0558

for 10-Et-5-DIAll at 17 000, 20 700, 24 900, 28 300 and 30 300 cm^{-1}. Note that there are several lower-energy transitions (Table 6), which could not be probed in the experimental spectrum, because of the limitations of the flash-photolysis equipment.

Figure 6 shows the shape of the highest occupied molecular orbitals (HOMO) and the lowest unoccupied molecular orbitals (LUMO) of 8-Me-5-DAll, 9-Me-5-DAll and 10-Et-5-DIAll, mainly involved in the lowest singlet-singlet transitions, which are dominant in the $S_0 \rightarrow S_1$ transition. Additionally, we show in Fig. 7 the shape of the highest occupied molecular orbitals (HOMO) and the lowest unoccupied molecular orbitals (LUMO) of 9-Me-5-DAll, involved also in the higher singlet-singlet transitions, namely $S_0 \rightarrow S_2$, and $S_0 \rightarrow S_3$, which are closely located. The latter have dominant contribution from the HOMO—2 → LUMO (n,π*) and from the HOMO—1 → LUMO excitations (π,π*).

Unfortunately, there are no data available for comparison, concerning the shape of the HOMO and LUMO molecular orbitals calculated for the derivatives of 5-deazalloxazine.

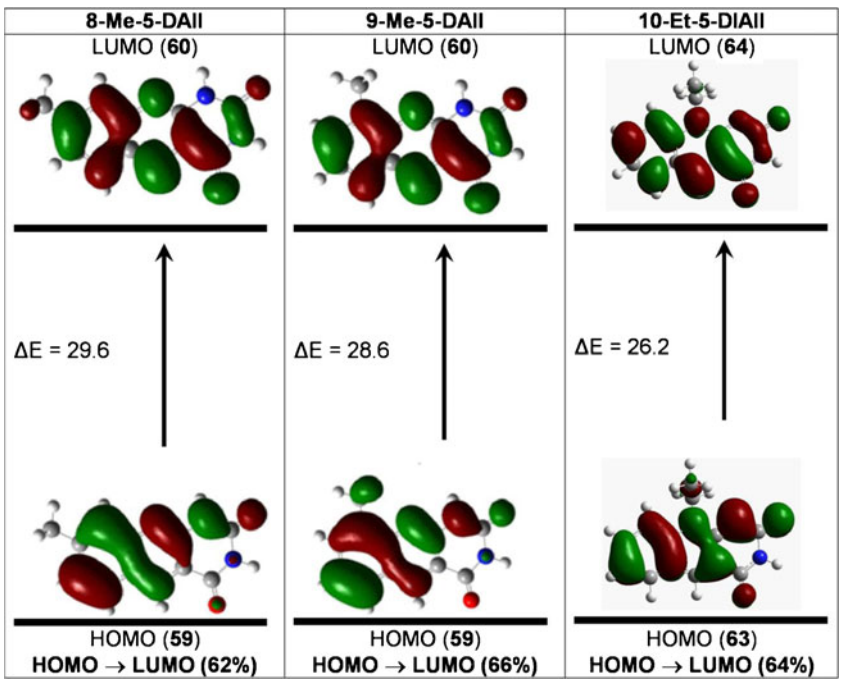

Fig. 6 The shape of the highest occupied molecular orbitals (HOMO) and the lowest unoccupied molecular orbitals (LUMO) for 8-Me-5-DAll, 9-Me-5-DAll and 10-Et-5-DIAll, mainly involved in the lowest singlet-singlet transitions. The isosurfaces correspond to the wave function value of±0.02

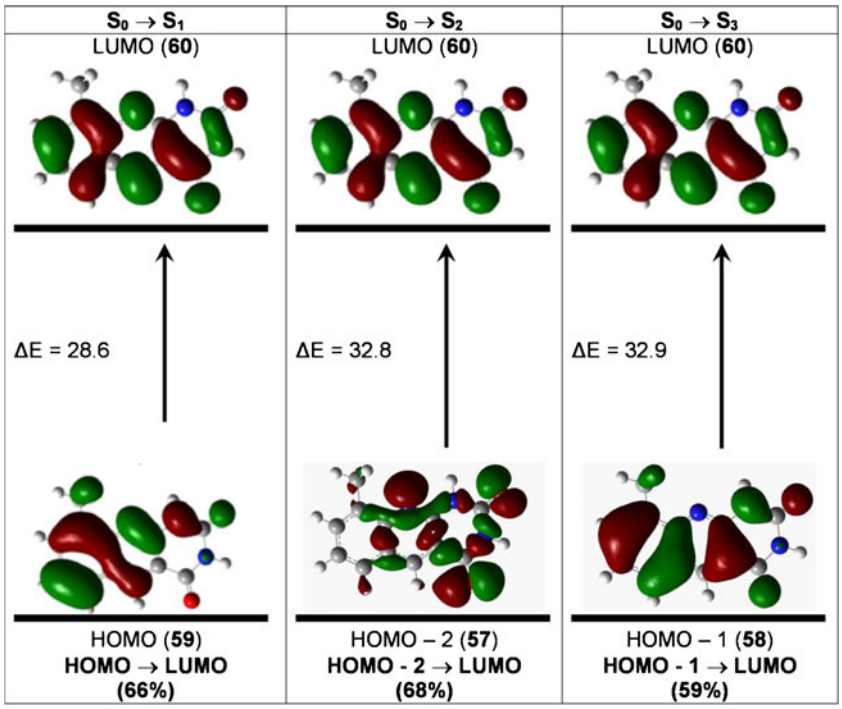

Fig. 7 The shape of the orbitals for 9-Me-5-DAll, mainly involved in the $S_0 \rightarrow S_1$, $S_0 \rightarrow S_2$ and $S_0 \rightarrow S_3$ transitions. The isosurfaces correspond to the wave function value of±0.02

We found a different picture for alloxazines, because the derivatives of 8-methylalloxazine and 9-methylalloxazine have a dominant contribution from the HOMO—2→LUMO excitation and is assigned as an n,π* transition. However, such n,π* transitions are accompanied by closely-located π, π* transitions with a dominant contribution from the HOMO→LUMO excitation [34].

We can compare the frontier orbitals calculated for 10-Et-5-DIAll with those calculated for derivatives of isoalloxazines and 5-deaza-isoalloxazines. For both classes of compounds, the $S_0 \rightarrow S_1$ transition is predicted having the dominant contribution from the HOMO→LUMO excitation, and can be interpreted as an allowed π, π* transitions [60].

Interestingly, the shape of HOMO and LUMO orbitals of the derivatives of isoalloxazine and 5-deaza-isoalloxazine is almost the same. This, for example, is true for 3-ethyl-lumiflavin, lumiflavin, 5-deazariboflavin, and 5-deazalumiflavin [23, 45, 61]. The shapes of the molecular orbitals of 10-Et-5-DIAll also obey the same rule.

In Fig. 8 we show the atomic charges of neutral forms of 8-Me-5-DAll, 9-Me-5-DAll and 10-Et-5-DIAll in the ground (S_0) and in the first excited singlet state (S_1) in the gas phase determined by the NBO population analysis. Centers with partial negative charges include N(1), N(3) and N(10) nitrogen atoms and O(2) and O(4) oxygen atoms of the carbonyl groups. The magnitudes of the negative charges at heteroatoms in the ground state of 8-Me-5-DAll and in 9-Me-5-DAll are as follows, from lower to higher: N(10), O(4), O(2), N(1), and N(3). The atoms with the largest positive charge are the carbonyl carbon atoms with charge at C(2) larger than that at C(4), for both compounds. The positive charges at the two hydrogen atoms of the N-H groups are almost the same (Fig. 8). Interestingly, though the oxygen atoms have quite large negative charges in the ground state, they are still not involved in the hydrogen bonds, as we concluded from the solvatochromic experiments.

Among the heteroatoms in 8-Me-5-DAll and 9-Me-5-DAll, the largest change of the net electron density comparing S_0 and S_1 states occurs on the O(4) oxygen atom. The results of NBO analysis for 8-Me-5-DAll and 9-Me-5-DAll indicate that the negative charge at O(4) is lower in the S_1 compared to the S_0 state. On the contrary, the negative charge at O(2) of both compounds is higher in the S_1 as compared to the S_0 state, although the changes are small. The largest growth of the negative charge at heteroatoms upon excitation occur on the N(10) nitrogen atom of both compounds. After excitation, the electron density at hydrogen atoms of the N-H groups changes slightly for both molecules, although we noted an increase in the N(1)—H bond polarity in the excited state.

More significant differences in the electron density on certain atoms between the ground and the first excited singlet state are observed for 10-Et-5-DIAll. Namely, all nitrogen atoms have a lower electron density in the first singlet excited state. Interestingly, the N(1) atom in the ground state has the largest negative charge among all of the heteroatoms. Therefore, we assume that this atom is mainly involved in the hydrogen-bonded complex in the ground state. However, the O(2), and O(4) oxygen atoms become more negative than the N(1) nitrogen atom in the S_1 state.

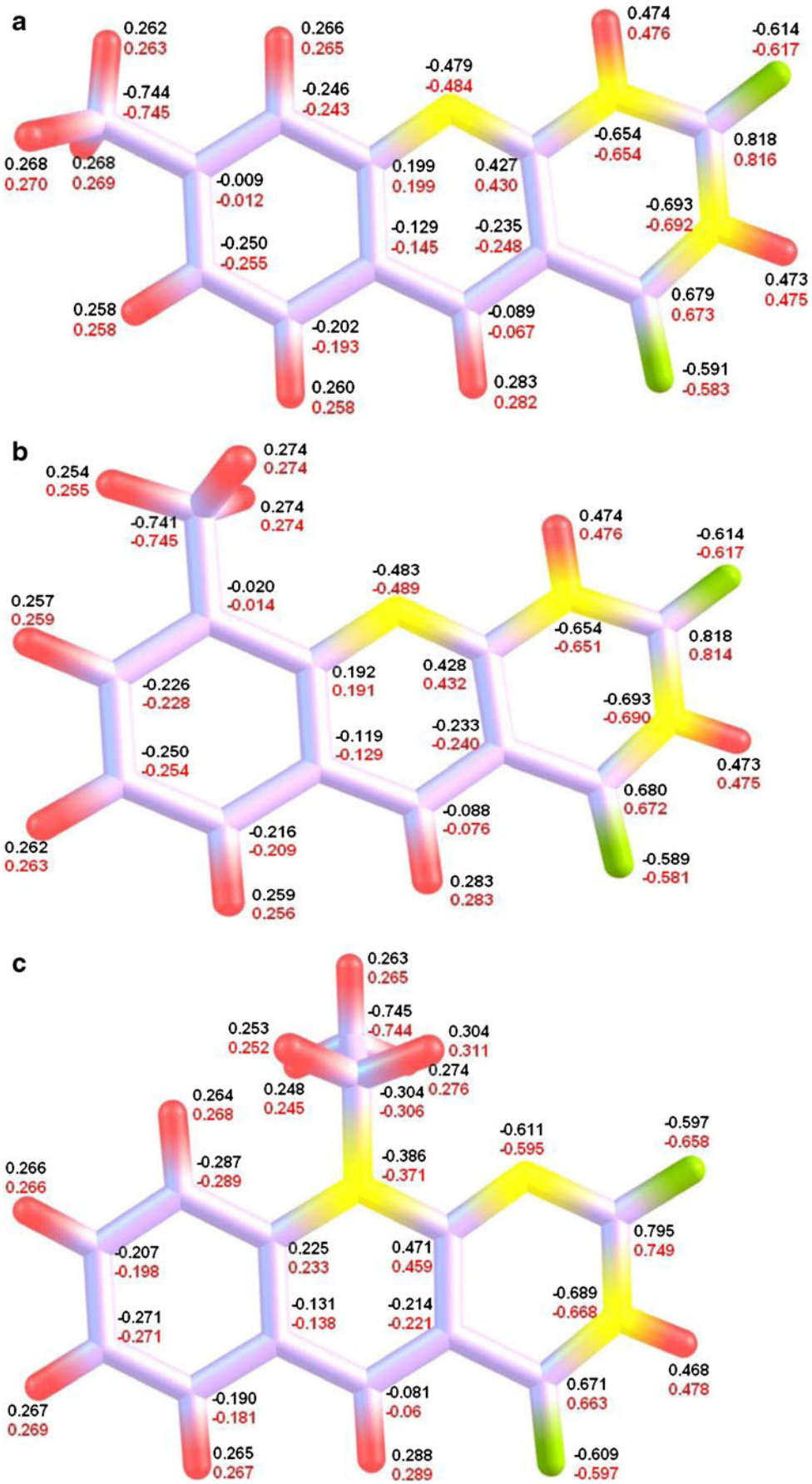

Fig. 8 Atomic charges of neutral form of 8-Me-5-DAll, 9-Me-5-DAll and 10-Et-5-DIAll in the ground (S_0) and in the first excited singlet state (S_1) in the gas phase determined by the NBO population analysis, respectively: **a** 8-Me-5DAll, **b** 9-Me-5DAll, **c** 10-Et-5DIAll, S_0—black, S_1—red

Conclusions

We described spectral, photophysical and solvatochromic properties of derivative of 5-deaza-isoalloxazine and two monomethyl derivatives of 5-deazaalloxazine, using both experimental and theoretical methods. We found that although the structures of alloxazines and 5-deazaalloxazines are similar, there is some difference in properties, including the fluorescence lifetimes and quantum yields, which are higher for 5-deazaalloxazines as compared to their "aza" analogues. The theoretical calculations indicate that the lowest-energy transitions has π,π^* character, being unaccompanied by closely-located n,π^* transitions, as is the case for alloxazines.

The energy of the lowest-energy absorption transition calculated using TD-DFT methods for isolated molecules is very close to that estimated for the same molecules in the gas phase (A_0 parameter) using the Catalán scale; this is especially true for 8-methyl-5-deazaalloxazine.

Solvatochromic studies show that hydrogen bonds are formed both in the ground and in the excited states for 8-methyl-5-deazaalloxazine and 9-methyl-5-deazaalloxazine but only in the ground state for 10-ethyl-5-deaza-isoalloxazine.

We also investigated the triplet states of the target compounds. We found that the lowest triplet excited state has π,π^* character.

Acknowledgments This study was supported by the research grant DEC-2012/05/B/ST4/01207 from The National Science Centre of Poland (NCN). All of the calculations were performed at the PL-Grid project.

References

1. Chastain J, McCormick DB (1991) In: Müller F (ed) Chemistry and biochemistry of flavoenzymes. CRC Press, Boston, pp 196–200
2. Silva E, Edwards AM (2006) Flavins: photochemistry and photobiology; comprehensive series in photochemistry and photobiology. The Royal Society of Chemistry, Cambridge, 6
3. Walsh C (1986) Naturally occurring 5-deazaflavin coenzymes: biological redox roles. Acc Chem Res 19:216–221
4. Losi A, Silva E (2006) Flavin-based photoreceptors in bacteria. In: Edwards AM (ed) Flavin photochemistry and photobiology. Elsevier, Amsterdam, pp 223–269
5. Glas AF, Maul MJ, Cryle M, Barends TRM, Schneider S, Kaya E, Schlichting I, Carell T (2009) The Archaeal cofactor F_0 is a light-harvesting antenna chromophore in eukaryotes. PNAS 1006:11540–11545
6. Bystrykh LV, Govorukhina NI, Dijkhuizen L, Duine JA (1997) Tetrazolium-dye-linked alcohol dehydrogenase of the methylotrophic actinomycete Amycolatopsis methanolica is a three-component complex. Eur J Biochem 247:280–287
7. Schäfer G, Engelhard M, Muller V (1999) Bioenergetics of the Archaea. Microbiol Mol Biol Rev 63:570–620
8. Hemmerich P, Massey V, Fenner H (1977) Flavin and 5-deazaflavin: a chemical evaluation of 'modified' flavoproteins with respect to the mechanisms of redox biocatalysis. FEBS Lett 84:5–21
9. Ali HI, Ashida N, Nagamatsu T (2008) Antitumor studies. Part 4: design, synthesis, antitumor activity, and molecular docking study of novel 2-substituted 2-deoxoflavin-5-oxides, 2-deoxoalloxazine-5-oxides, and their 5-deaza analogs. Bioorg Med Chem 16:922–940
10. Ikeuchi Y, Sumiya M, Kawamoto T, Akimoto N, Mikata Y, Kishigami M, Yano S, Sasaki T, Yoneda F (2000) Synthesis and antitumor activities of novel 5-deazaflavin-sialic acid conjugate molecules. Bioorg Med Chem 8:2027–2035
11. Kanaoka Y, Ikeuchi Y, Kawamoto T, Besso K, Akimoto N, Mikata Y, Nishida M, Yano S, Tasaki S, Yoneda F (1998) Synthesis and evaluation of nitro 5-deazaflavinpyrrolecarboxamide(s) hybrid molecules as novel DNA targeted bioreductive antitumor agents. Bioorg Med Chem 6:301–314
12. Kawamoto M, Ikeuchi Y, Hiraki J, Eikyu Y, Shimizu K, Tomishima M, Bessho K, Yoneda F, Mikata Y, Nishida M, Ikehara K, Sasaki T (1995) Synthesis and evaluation of nitro 5-deazaflavins as novel bioreductive antitumor agents. Bioorg Med Chem Lett 5:2109–2114
13. Wilson JM, Henderson G, Black F, Sutherland A, Ludwig RL, Vousden KH, Robins DJ (2007) Synthesis of 5-deazaflavin derivatives and their activation of p53 in cells. Bioorg Med Chem 15:77–86
14. Stover CK, Warrener P, Van Devanter DR, Sherman DR, Arain TM, Langhorne MH, Anderson SW, Towell JA, Yuan Y, McMurray DN, Kreiswirth BN, Barry CE, Baker WR (2000) A small-molecule nitroimidazopyran drug candidate for the treatment of tuberculosis. Nature 405:962–966
15. Koziołowa A, Visser NV, Kozioł J, Szafran MM (1996) Phototautomerism of 5-deazalumichrome (in the presence of acetic acid). J Photochem Photobiol A 93:157–163
16. Yagi K, Ohishi N, Nishimoto K, Choi JD, Song P-S (1980) Effect of hydrogen bonding on electronic spectra and reactivity of flavins. Biochemistry 19(1553–1):557
17. Neiss C, Saalfrank P, Parac M, Grimme S (2003) Quantum chemical calculation of excited states of flavin-related molecules. J Phys Chem A 107:140–147
18. Sikorska E, Khmelinskii IV, Koput J, Bourdelande JL, Sikorski M (2004) Electronic structure of isoalloxazines in their ground and excited states. J Mol Struct 697:137–141
19. Sikorska E, Khmelinskii IV, Kubicki M, Prukała W, Hoffmann M, Machado IF, Ferreira LFV, Karolczak J, Worrall DR, Krawczyk A, Insińska-Rak M, Sikorski M (2006) In search of excited-state proton transfer in the lumichrome dimer in the solid state: theoretical and experimental approach. J Phys Chem A 110:4638–4648
20. Sikorska E, Khmelinskii IV, Hoffmann M, Machado IF, Ferreira LFV, Dobek K, Karolczak J, Krawczyk A, Insińska-Rak M, Sikorski M (2005) Ground- and excited-state double proton transfer in lumichrome/acetic acid system: theoretical and experimental approach. J Phys Chem A 109:11707–11714
21. Sikorska E, Khmelinskii IV, Bednarek A, Williams SL, Worrall DR, Herance JR, Bourdelande JL, Nowacka G, Koput J, Sikorski M (2004) Spectroscopy and photophysics of 6,8-dimethyl-alloxazine. Experimental and theoretical study. Pol J Chem 78:2163–2173
22. Sikorska E, Khmelinskii IV, Nowacka G, Koput J, Sikorski M (2005) Spectroscopy and photophysics of cyanoalloxazines. Theoretical study. J Mol Struc (Theochem) 722:51–56
23. Insińska-Rak M, Sikorska E, Bourdelande JL, Khmelinskii IV, Prukała W, Dobek K, Karolczak J, Machado IF, Ferreira LFV, Komasa A, Worrall DR, Sikorski M (2006) Spectroscopy and photophysics of flavin-related compounds: 5-deaza-riboflavin. J Mol Struct 783:184–190
24. Salzmann S, Martinez-Junza V, Zorn B, Braslavsky SE (2009) Photophysical properties of structurally and electronically modified flavin derivatives determined by spectroscopy and theoretical calculations. J Phys Chem A 113:9365–9375
25. Nishigaki S, Sato J, Shimizu K, Furukawa K, Senga K, Yoneda F (1980) Synthesis of 1,3-dimethylpyrimido[4,5-b]quinoline-2,4(1H,3H)-diones (1,3-dimethyl-5-deazaalloxazines) and related compounds via the intramolecular cycloaddition of azahexatrienes. Chem Pharm Bull 28:142–149

26. Nagamatsu T, Hashiguchi Y, Yoneda F (1984) A new, general, and convenient synthesis of 5-deazaflavins (5-deazaisoalloxazines) and bis-(5-deazaflavin-10-yl)alkanes. J Chem Soc Perkin Trans 1:561–565
27. Goldner H, Dietz G, Carstens E (1966) Neue reaktionen mit nitrosouracilderivaten.4. Die synthese von alloxazinen und alloxazin-5-N-oxiden. Liebigs Ann Chem 694:142–145
28. Ali HI, Ashida N, Nagamatsu T (2007) Antitumor studies. Part 3: design, synthesis, antitumor activity, and molecular docking study of novel 2-methylthio-, 2-amino-, and 2-(N-substituted amino)-10-alkyl-2-deoxo- 5-deazaflavins. Bioorg Med Chem 15:6336–6352
29. Sikorska E, Khmelinskii IV, Prukała W, Williams SL, Patel M, Worrall DR, Bourdelande JL, Koput J, Sikorski M (2004) Spectroscopy and photophysics of lumiflavins and lumichromes. J Phys Chem A 108:1501–1508
30. From website: www.jyhoriba.co.uk
31. Pędzinski T, Markiewicz A, Marciniak B (2009) Photosensitized oxidation of methionine derivatives. Laser flash photolysis studies. Res Chem Intermed 35:497–506
32. ACD/ChemSketch; version 4.55; Advanced Chemistry; Development Inc., Toronto, Canada. Ed., 2000
33. Prukała D, Sikorska E, Koput J, Khmelinskii IV, Karolczak J, Gierszewski M, Sikorski M (2012) Acid–base equilibriums of lumichrome and its 1-methyl, 3-methyl, and 1,3-dimethyl derivatives. J Phys Chem A 116:7474–7490
34. Bruszyńska M, Sikorska E, Komasa A, Khmelinskii IV, Ferreira LFV, Hernando J, Karolczak J, Kubicki M, Bourdelande JL, Sikorski M (2009) Electronic structure and spectral properties of selected trimethyl-alloxazines: combined experimental and DFT study. Chem Phys 361:83–93
35. Neiss C, Saalfrank P (2003) Ab initio quantum chemical investigation of the first steps of the photocycle of phototropin: a model study. Photochem Photobiol 77:101–109
36. Sun M, Moore TA, Song P-S (1972) Molecular luminescence studies of flavins. I. The excited states of flavins. J Am Chem Soc 94:1730–1740
37. Platenkamp RJ, Palmer MH, Visser AJWG (1987) Ab initio molecular orbital studies of closed shell flavins. Eur Biophys J 14:393–402
38. Sikorska E, Khmelinskii IV, Prukała W, Williams SL, Worrall DR, Bourdelande JL, Bednarek A, Koput J, Sikorski M (2004) Spectroscopy and photophysics of 9-methylalloxazine. Experimental and theoretical study. J Mol Struct 689:121–126
39. Becke AD (1993) Density-functional thermochemistry. III. The role of exact exchange. J Chem Phys 98:5648–5652
40. Ditcrfield R, Herre WJ, Pople JA (1971) Self consistent molecular orbital methods. IX. An extended gaussian type basis for molecular orbital studies of organic molecules. J Chem Phys 54:724–728
41. Lee CT, Yang WT, Parr RG (1988) Development of the colle-salvetti correlation-energy formula into a functional of the electron density. Phys Rev B 37:785–789
42. Trucks GW, Schlegel HB, Scuseria GE, Robb MA, Cheeseman JR, Montgomery AJ Jr, Vreven T, Kudin KN, Burant JC, Millam JM (2003) Gaussian 03, revision B.05. Gaussian Inc., Wallingford
43. Kozioł J (1969) Studies on flavins in organic solvents. III. Spectral behavior of lumiflavin. Photochem Photobiol 9:45–54
44. Sikorska E, Khmelinskii IV, Koput J, Sikorski M (2004) Electronic structure of lumiflavin and its analogues in their ground and excited states. J Mol Struct (Theochem) 676:155–160
45. Sikorska E, Herance JR, Bourdelande JL, Khmelinskii IV, Williams SL, Worrall DR, Nowacka G, Komasa A, Sikorski M (2005) Spectroscopy and photophysics of flavin-related compounds: 3-ethyl-lumiflavin. J Photochem Photobiol A 170:267–272
46. Catalán J (2009) Toward a generalized treatment of the solvent effect based on four empirical scales: dipolarity (SdP, a new scale), polarizability (SP), acidity (SA), and basicity (SB) of the medium. J Phys Chem B 113:5951–5960
47. Lakowicz JR (1999) Principles of fluorescence spectroscopy, 2nd edn. New York
48. Lippert E (1957) Spektroskopische bestimmung des dipolmomentes aromatischer verbindungen im ersten angeregten singulettzustand. Z Elektrochem 61:962–975
49. Reynolds L, Gardecki JA, Frankland SJV, Horng ML, Maroncelli M (1996) Dipole solvation in nondipolar solvents—experimental studies of reorganization energies and solvation dynamics. J Phys Chem 100:10337–10354
50. Moyon N, Mitra S (2011) Fluorescence solvatochromism in lumichrome and excited-state tautomerization: a combined experimental and DFT study. J Phys Chem A 115:2456–2464
51. Catalán J, López V, Pérez P, Matin-Villamil R, Rodriguez JG (1995) Progress towards a generalized solvent polarity scale: the solvatochromism of 2-(dimethylamino)-7-nitrofluorene and its homomorph 2-fluoro-7-nitrofluorenee. Liebigs Ann 241–252
52. Sikorska E, Szymusiak H, Khmelinskii IV, Koziołowa A, Spanget-Larsen J, Sikorski M (2003) Spectroscopy and photophysics of alloxazines studied in their ground and first excited singlet states. J Photochem Photobiol A 158:45–53
53. Sikorska E, Khmelinskii IV, Kubicki M, Prukała W, Nowacka G, Siemiarczuk A, Koput J, Ferreira LFV, Sikorski M (2005) Hydrogen-bonded complexes of lumichrome. J Phys Chem A 105:1785–1794
54. Sikorska E, Bourdelande JL, Worrall DR, Sikorski M (2003) Photophysics of lumichrome and its analogs. Pol J Chem 77:65–73
55. Sikorska E, Sikorski M, Steer RP, Wilkinson F, Worrall DR (1998) Efficiency of singlet oxygen generation by alloxazines and isoalloxazines. J Chem Soc Faraday Trans 94:2347–2353
56. Martin CB, Shi XF, Tsao ML, Karweik D, Brooke J, Hadad CM, Platz MS (2002) The photochemistry of riboflavin tetraacetate and nucleosides. A study using density functional theory, laser flash photolysis, fluorescence, UV–vis, and time resolved infrared spectroscopy. J Phys Chem B 106:10263–10271
57. Martin CB, Tsao ML, Hadad CM, Platz MS (2002) The reaction of triplet flavin with indole. A study of the cascade of reactive intermediates using density functional theory and time resolved infrared spectroscopy. J Am Chem Soc 124:7226–7234
58. Rodriguez-Otero J, Martinez-Nunez E, Pena-Gallego A, Vazquez SA (2002) The role of aromaticity in the planarity of lumiflavin. J Org Chem 67:6347–6352
59. Sikorska E, Khmelinskii IV, Worrall DR, Koput J, Sikorski M (2004) Spectroscopy and photophysics of iso- and alloxazines. Experimental and theoretical study. J Fluoresc 14:57–64
60. Kowalczyk M, Sikorska E, Khmelinskii IV, Komasa J, Insińska-Rak M, Sikorski M (2005) Spectroscopy and photophysics of flavin-related compounds: isoalloxazines. J Mol Struct (Theochem) 756: 47–54
61. Salzmann S, Tatchen J, Marian CM (2008) The photophysics of flavins: what makes the difference between gas phase and aqueous solution. J Photochem Photobiol A 198:221–231